

ASR-INDUCED ANISOTROPY IN THE MECHANICAL PROPERTIES OF CONCRETE

Anca Ferche
Frank Vecchio

March 29th, 2022



“6th Street Viaduct Seismic Improvement Project,” *California Department of Transportation and City of Los Angeles*, 2011.



ASR-INDUCED ANISOTROPY IN THE MECHANICAL PROPERTIES OF CONCRETE

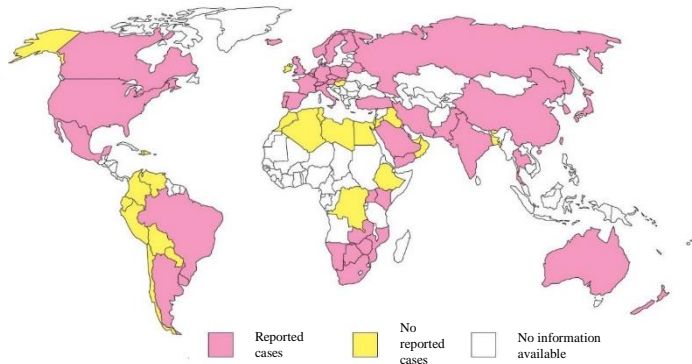
OUTLINE

1. INTRODUCTION
2. MECHANICAL PROPERTIES OF ASR-AFFECTED CONCRETE
 - EXPERIMENTAL PROGRAM
 - ANALYTICAL PROGRAM
3. VALIDATION STUDIES
4. CONCLUSIONS

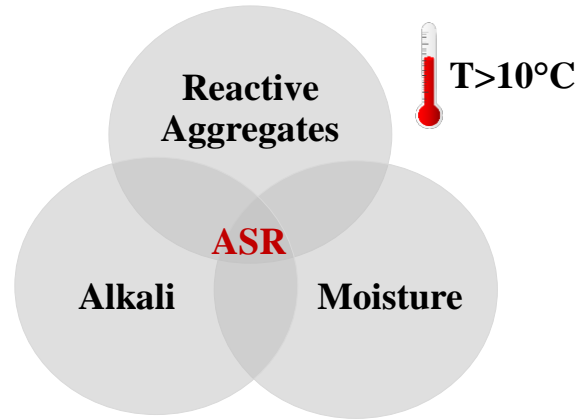


1. INTRODUCTION

ALKALI-SILICA REACTION

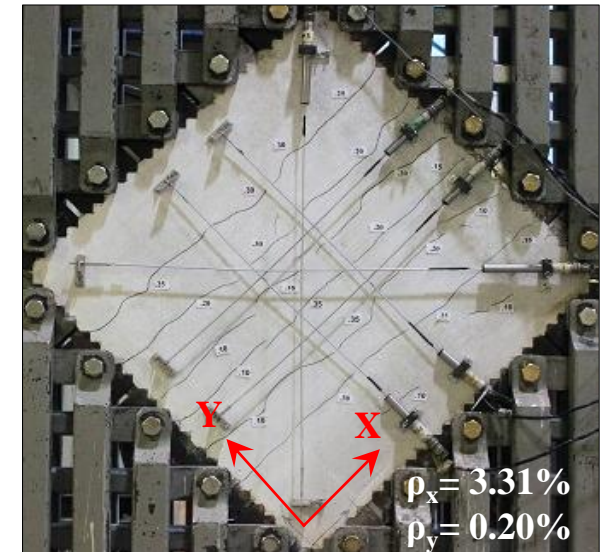


(adapted from Sims and Poole, 2017)



Influencing Factors

- Temperature,
- Water availability,
- Alkali content,
- Type of reactive aggregates,
 - Aggregate size,
 - Air entrainment and porosity,
- Long-term stress level.



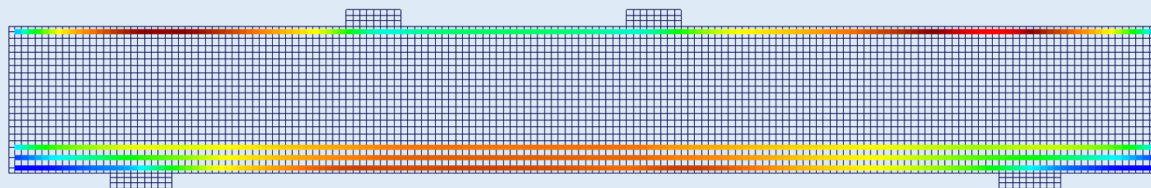
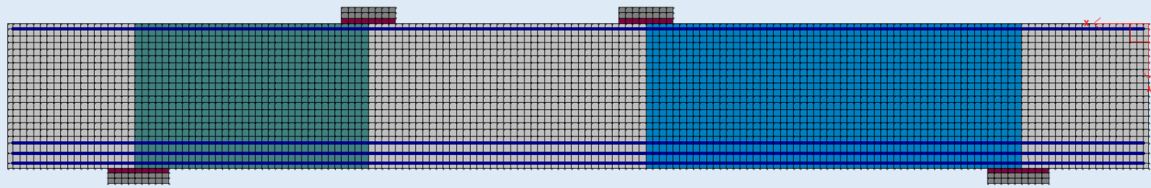
Source: "Condition assessment of an ASR-affected overpass after nearly 50 years in service," Sanchez et al., *Construction and Building Materials*, 2018.

ASR-Affected Dam, Norway
(Thomas et al., 2013)

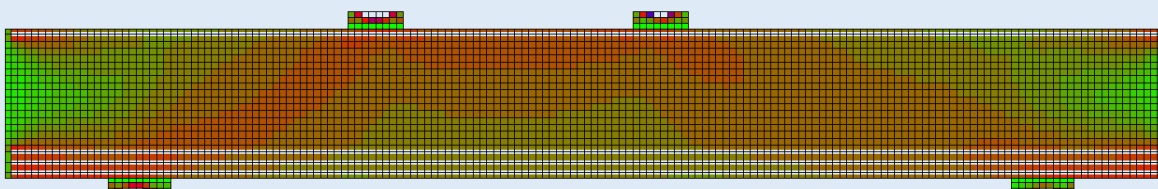
1. INTRODUCTION

ASR-RELATED STRUCTURAL IMPLICATIONS

EXPANSION-INDUCED PRESTRESS

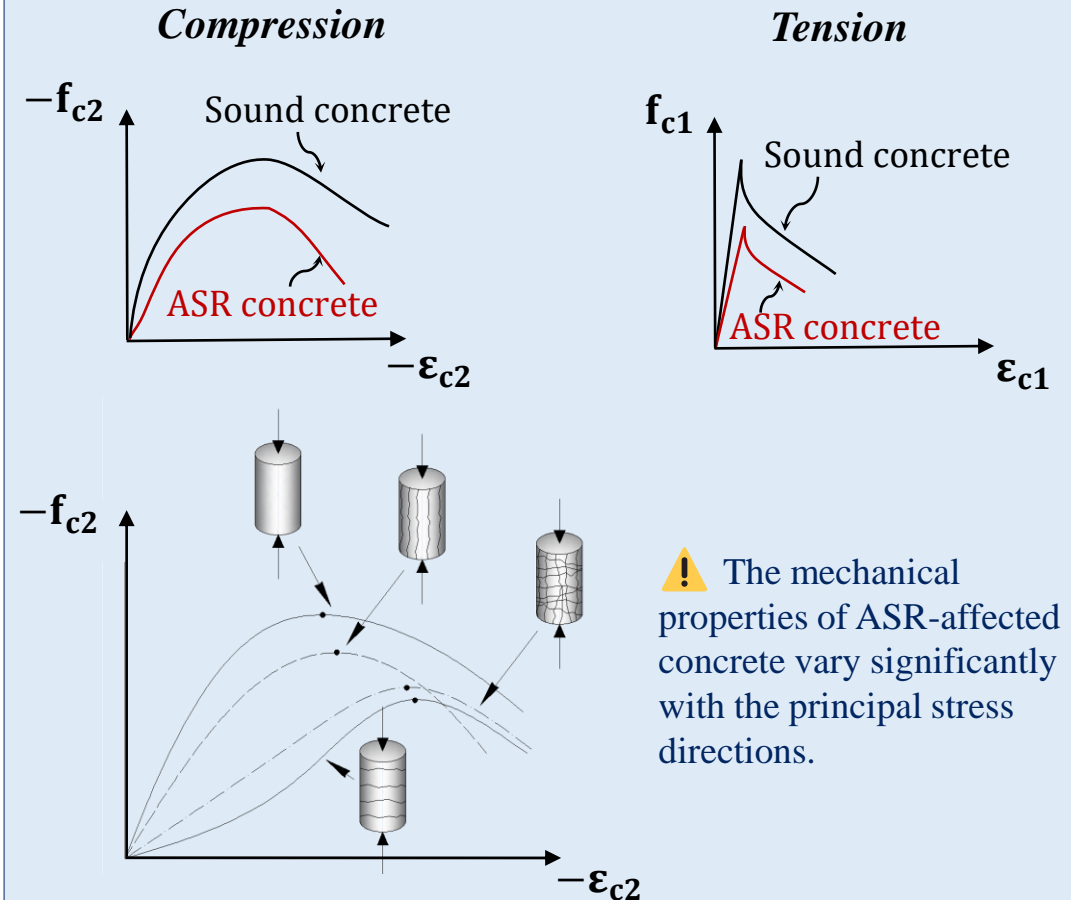


Longitudinal reinforcement stress



Concrete stress profile along the second principal direction

CONCRETE MECHANICAL PROPERTIES DEGRADATION



1. INTRODUCTION

NUMERICAL PROCEDURE FOR MODELING ASR-DAMAGED STRUCTURES

MODELING ASR EFFECTS WITH THE VECTOR PROGRAMS



VecTor2



& VecTor3

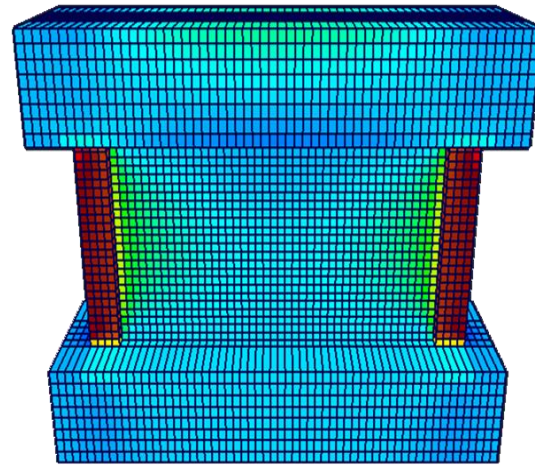


Stage 1: ASR Analysis

Evaluation of **ASR-induced strains** and **deterioration of mechanical properties** based on **long-term stress conditions**.

Required input for the ASR analysis:

- Unrestrained ASR expansion.
- Or characterization of the expansion & age of the structure.

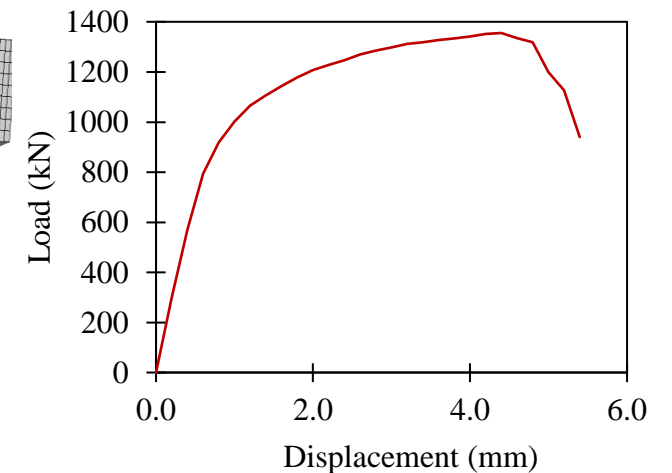
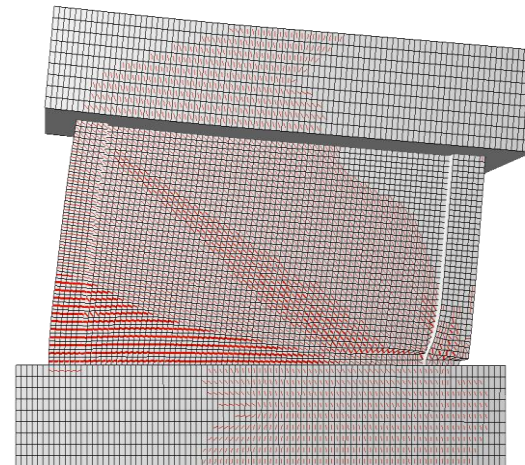


Outcomes:

- Stress and strain state in concrete and reinforcement caused by ASR expansion;
- Cracking characteristics.

Stage 2: Nonlinear Analysis

Nonlinear analysis considering the results obtained in Stage 1 to evaluate the **behavior** of the structure.



Outcomes:

- Load, deformation, and cracking response;
- Failure mode.

1. INTRODUCTION

NUMERICAL PROCEDURE FOR MODELING ASR-DAMAGED STRUCTURES

Stage 1: ASR Analysis → Evaluation of ASR-induced strains and deterioration of mechanical properties

ASR-Induced Strains Calculation

1. Uniform in each principal direction

2. Charlwood et al., 1992 model

Strains are independently evaluated in each direction, limited by confinement stress.

3. Curtis, 2014 model

A refined version of the Charlwood et al., 1992 model. Formulated based on field observations of the Mactaquac powerhouse.

4. Saouma and Perotti, 2006 model

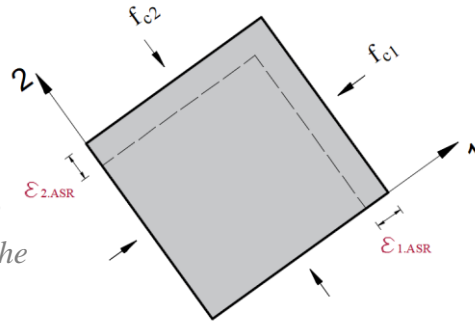
Expansion is treated as a volumetric strain.

5. Sellier et al., 2009 model

Strains are evaluated as a consequence of the gel pressure.

6. Gautam et al., 2017 model

Developed based on empirical data collected from ASR-affected multiaxially-loaded cube specimens.



Kinetics model

Deterioration of Mechanical Properties

1. ISE recommendations

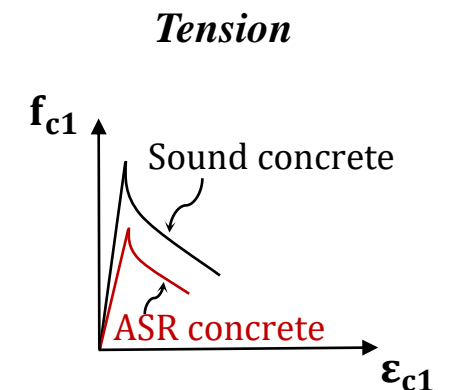
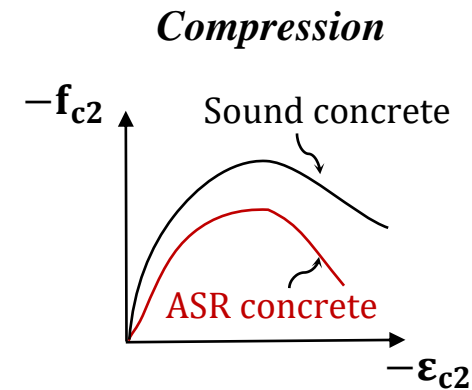
2. User-defined properties

3. Anisotropic model

4. Isotropic model

→ Reduction functions for:

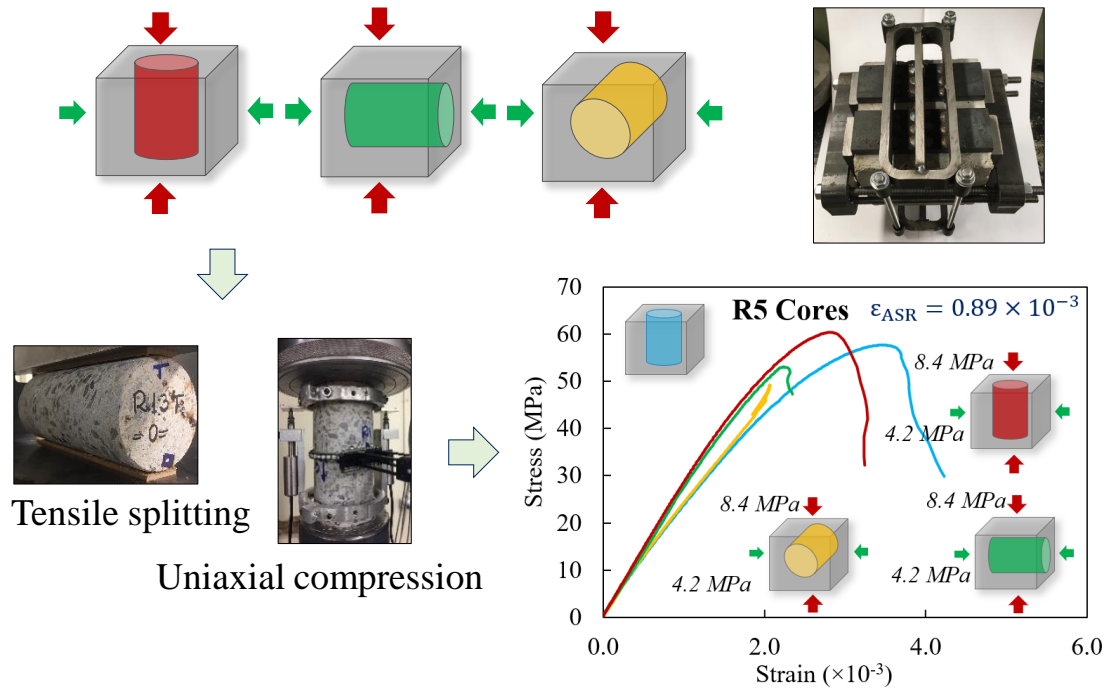
- Compressive strength
- Tensile strength
- Modulus of elasticity



2. MECHANICAL PROPERTIES OF ASR-AFFECTED CONCRETE

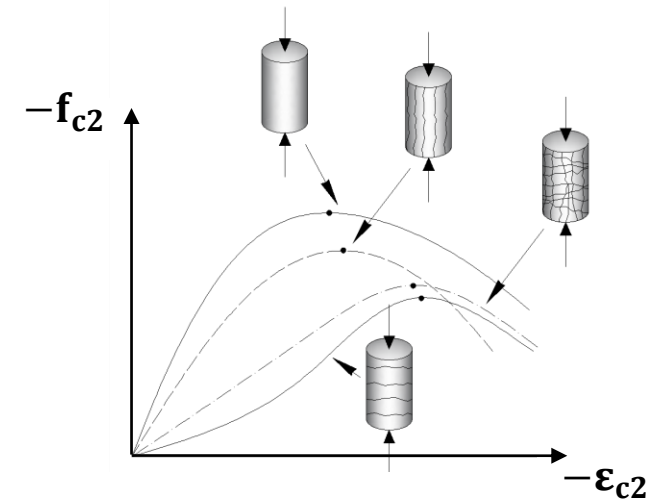
EXPERIMENTAL PROGRAM

Material-Level Study designed to capture the anisotropy of the mechanical properties of ASR-affected concrete.



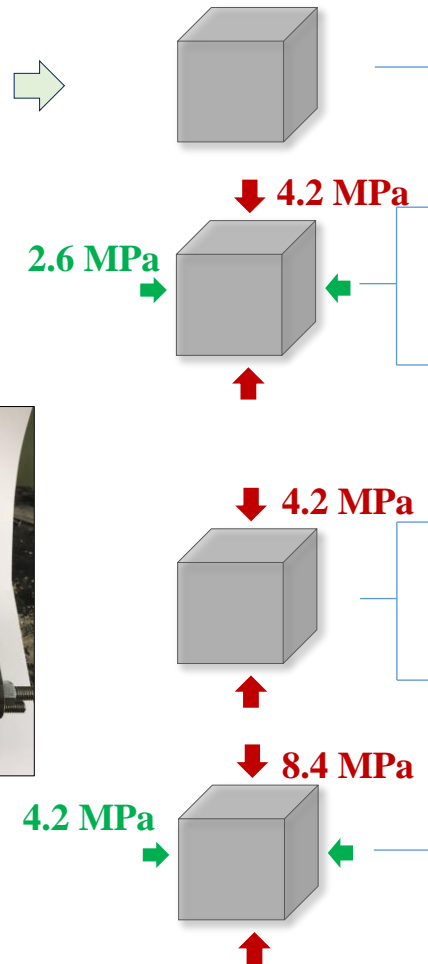
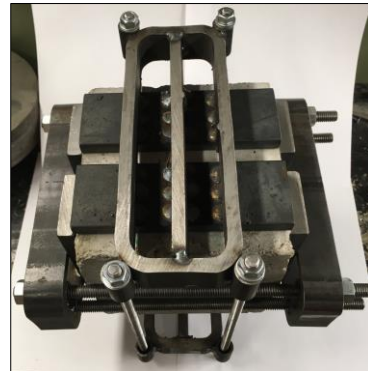
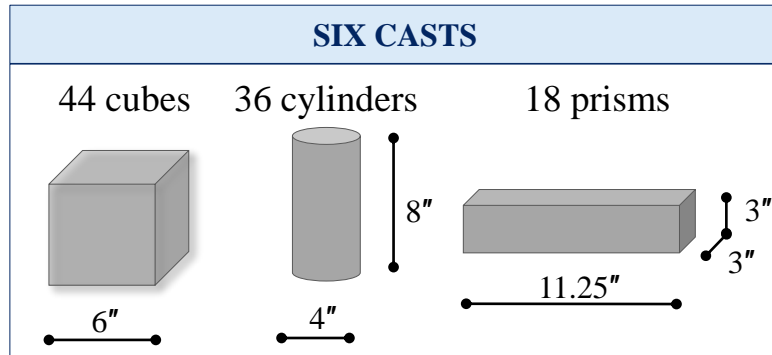
ANALYTICAL PROGRAM

Model for the Mechanical Properties of ASR-Affected Concrete developed to describe the directionality of the mechanical properties of ASR-affected concrete.



2. MECHANICAL PROPERTIES OF ASR-AFFECTED CONCRETE

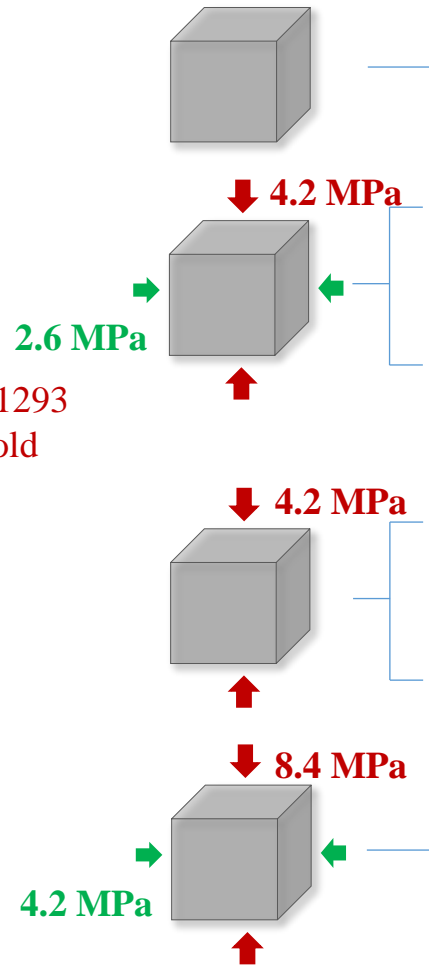
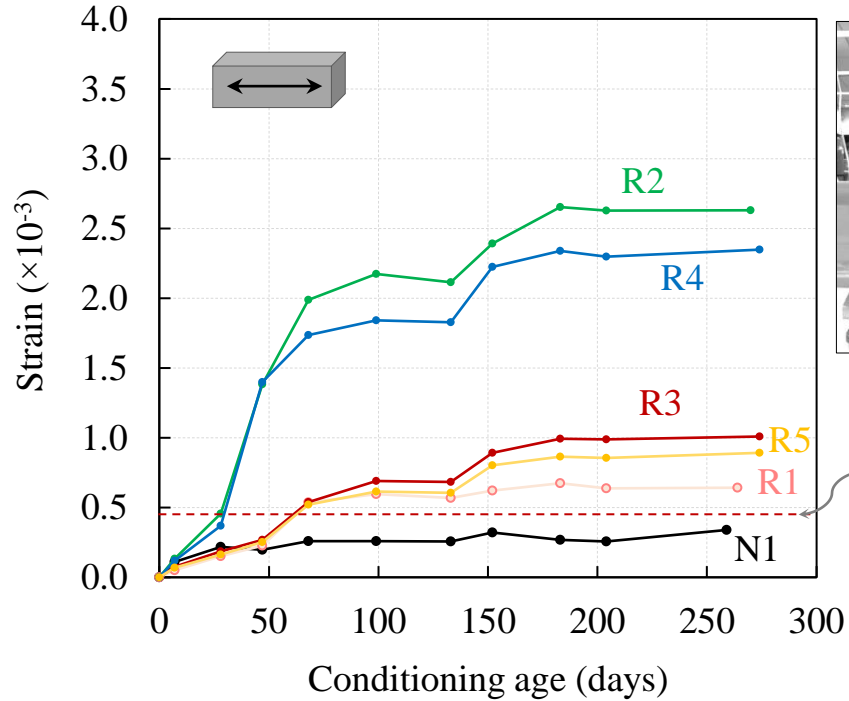
EXPERIMENTAL PROGRAM



Cubes set	# of cubes	σ_x (MPa)	σ_y (MPa)	σ_z (MPa)	Test method	Reactive aggregate
N1	4	0.00	0.00	0.00	Compression	None
	4	0.00	0.00	0.00	Tensile splitting	
R1	3	4.22	2.57	0.00	Compression	Spratt
	1	0.00	0.00	0.00	Tensile splitting	
	3	4.22	2.57	0.00		
R2	1	0.00	0.00	0.00	Compression	Jobe-Newman
	3	4.22	2.57	0.00	Tensile splitting	
	1	0.00	0.00	0.00		
R3	2	4.22	0.00	0.00	Compression	Spratt
	1	0.00	0.00	0.00	Tensile splitting	
	2	4.22	0.00	0.00		
R4	1	0.00	0.00	0.00	Compression	Jobe-Newman
	2	4.22	0.00	0.00	Tensile splitting	
	1	0.00	0.00	0.00		
R5	3	8.44	4.22	0.00	Compression	Spratt
	1	0.00	0.00	0.00	Tensile splitting	
	3	8.44	4.22	0.00		
	1	0.00	0.00	0.00		

2. MECHANICAL PROPERTIES OF ASR-AFFECTED CONCRETE

EXPERIMENTAL PROGRAM

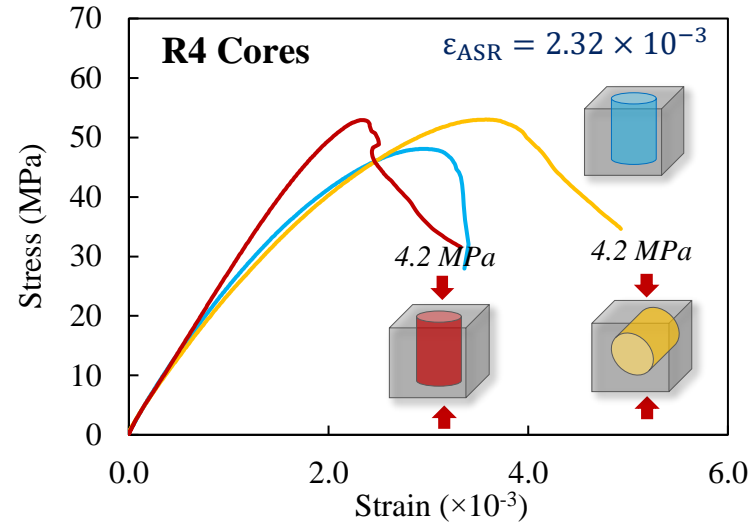
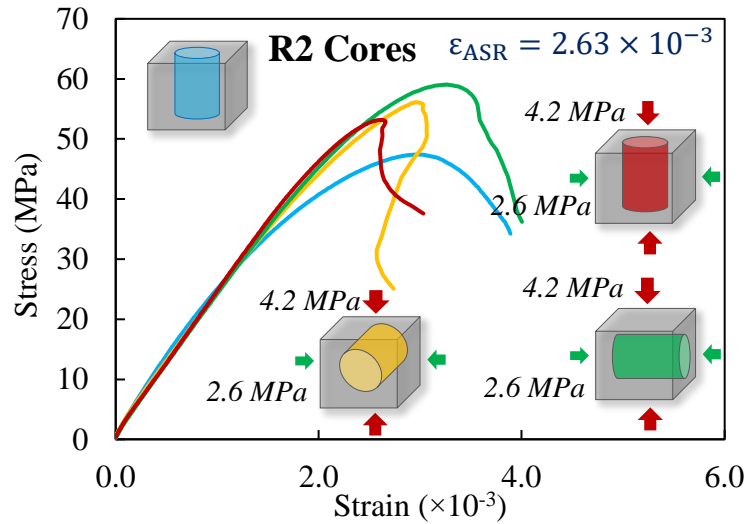


Cubes set	# of cubes	σ_x (MPa)	σ_y (MPa)	σ_z (MPa)	Test method	Reactive aggregate
N1	4	0.00	0.00	0.00	Compression	None
	4	0.00	0.00	0.00	Tensile splitting	
R1	3	4.22	2.57	0.00	Compression	Spratt
	1	0.00	0.00	0.00	Tensile splitting	
	3	4.22	2.57	0.00		
	1	0.00	0.00	0.00		
R2	3	4.22	2.57	0.00	Compression	Jobe-Newman
	1	0.00	0.00	0.00	Tensile splitting	
	3	4.22	2.57	0.00		
R3	2	4.22	0.00	0.00	Compression	Spratt
	1	0.00	0.00	0.00	Tensile splitting	
	2	4.22	0.00	0.00		
R4	1	0.00	0.00	0.00	Compression	Jobe-Newman
	2	4.22	0.00	0.00	Tensile splitting	
	2	4.22	0.00	0.00		
	1	0.00	0.00	0.00		
R5	3	8.44	4.22	0.00	Compression	Spratt
	1	0.00	0.00	0.00	Tensile splitting	
	3	8.44	4.22	0.00		
	1	0.00	0.00	0.00		

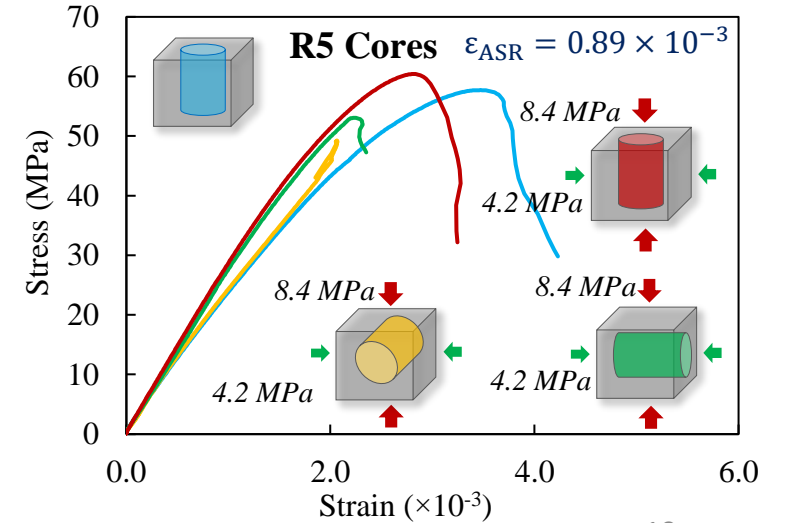
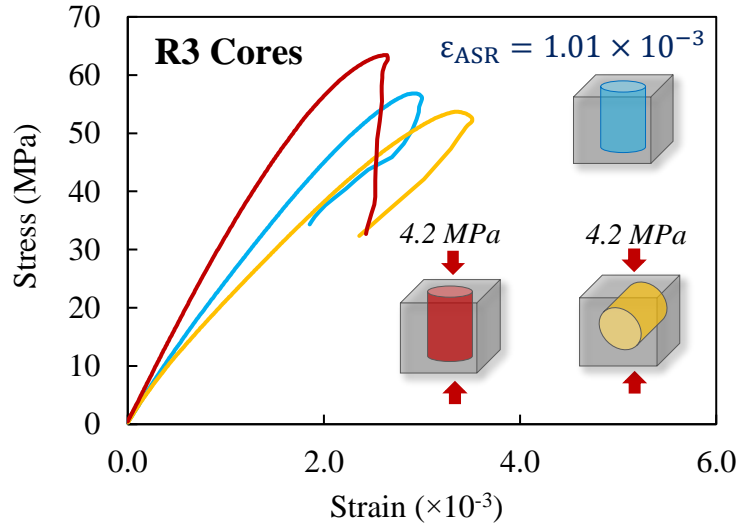
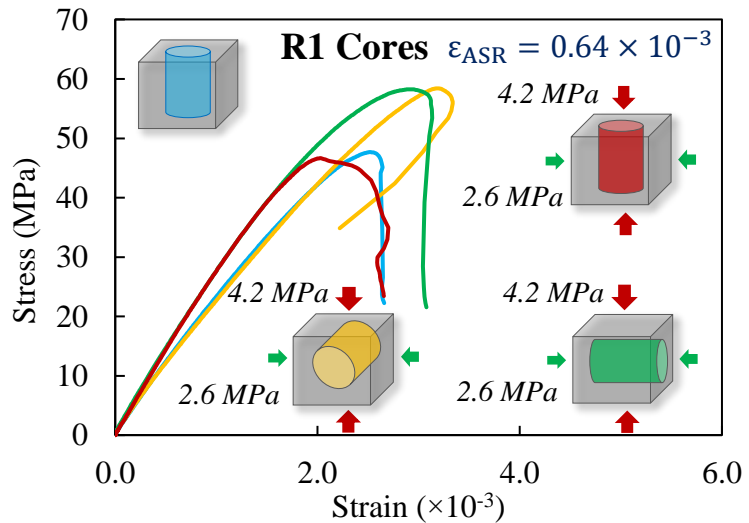
2. MECHANICAL PROPERTIES OF ASR-AFFECTED CONCRETE

EXPERIMENTAL PROGRAM

Jobe-Newman



Spratt



2. MECHANICAL PROPERTIES OF ASR-AFFECTED CONCRETE

EXPERIMENTAL PROGRAM

- ASR-induced deterioration affects differently the compressive strength, modulus of elasticity, and the tensile strength of concrete cured in stress free conditions.
- Long-term compressive stresses of 2.6 MPa and higher can essentially counteract the ASR-induced deterioration with respect to the concrete compressive strength along the restrained direction.
- The modulus of elasticity measured along the restrained directions is considerably more affected by ASR than the compressive strength.

Post-Conditioning Mechanical Properties

Core	f_p (MPa)	$\epsilon_p (\times 10^{-3})$	E_c (MPa)	f_{sp} (MPa)	μ
N1, non-reactive					
1	64.3	2.70	33800	5.19	0.16
2	63.1	2.56	33000	5.43	0.17
3	64.2	2.47	34200	5.20	0.16
Avg.	63.9	2.58	33700	5.27	0.17
R1, Spratt coarse aggregate: $\epsilon_{ASR}=0.64 \times 10^{-3}$					
0.0 MPa	58.4	3.19	22100	4.21	0.16
2.6 MPa	58.3	2.91	27400	4.34	0.14
4.2 MPa	46.6	2.02	28400	4.12	0.18
free	47.7	2.52	23500	3.59	0.15
R2, Jobe-Newman fine aggregate: $\epsilon_{ASR}=2.63 \times 10^{-3}$					
0.0 MPa	56.1	2.97	23600	3.82	0.19
2.6 MPa	59.0	3.25	23800	5.07	0.19
4.2 MPa	53.2	2.60	24000	3.97	0.20
free	47.4	2.97	25600	3.73	0.14
R3, Spratt coarse aggregate: $\epsilon_{ASR}=1.01 \times 10^{-3}$					
0.0 MPa	53.7	3.35	20600	4.03	0.11
4.2 MPa	63.4	2.64	32500	3.76	0.13
free	56.8	2.91	24400	3.47	0.11
R4, Jobe-Newman fine aggregate: $\epsilon_{ASR}=2.35 \times 10^{-3}$					
0.0 MPa	53.0	3.58	23200	4.16	0.17
4.2 MPa	52.9	2.33	26900	3.62	0.15
free	48.1	2.94	25500	4.01	0.13
R5, Spratt coarse aggregate: $\epsilon_{ASR}=0.89 \times 10^{-3}$					
0.0 MPa	49.2	2.07	24600	4.74	0.15
4.2 MPa	53.0	2.24	27000	3.81	0.17
8.4 MPa	60.4	2.81	28700	5.12	0.15
free	57.7	3.47	23300	3.86	0.14

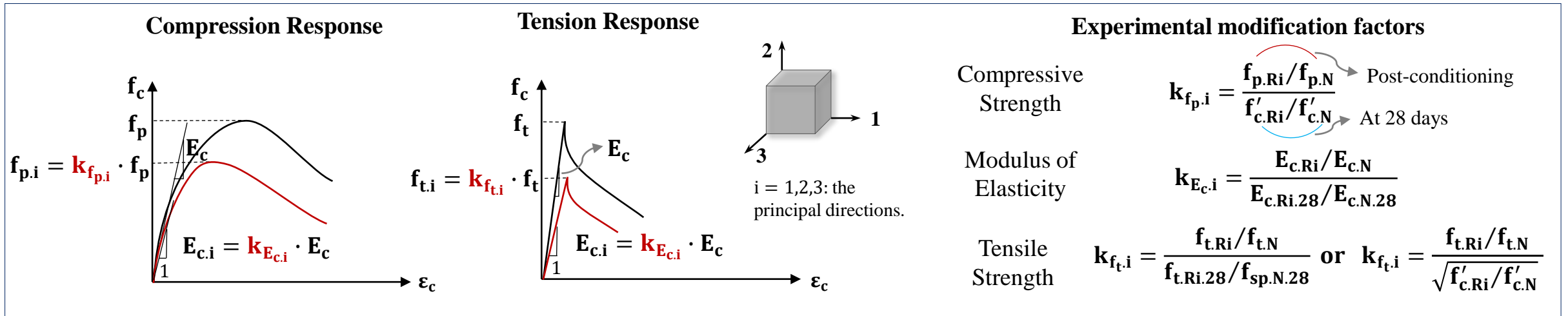
28-Day Mechanical Properties

Cast	f'_c (MPa)	$\epsilon_o (\times 10^{-3})$	E_c (MPa)
N1	45.9	2.69	30200
R1	40.1	2.30	30100
R2	42.7	2.54	31600
R3	38.6	2.45	29500
R4	46.6	2.73	31200
R5	38.0	2.42	28500

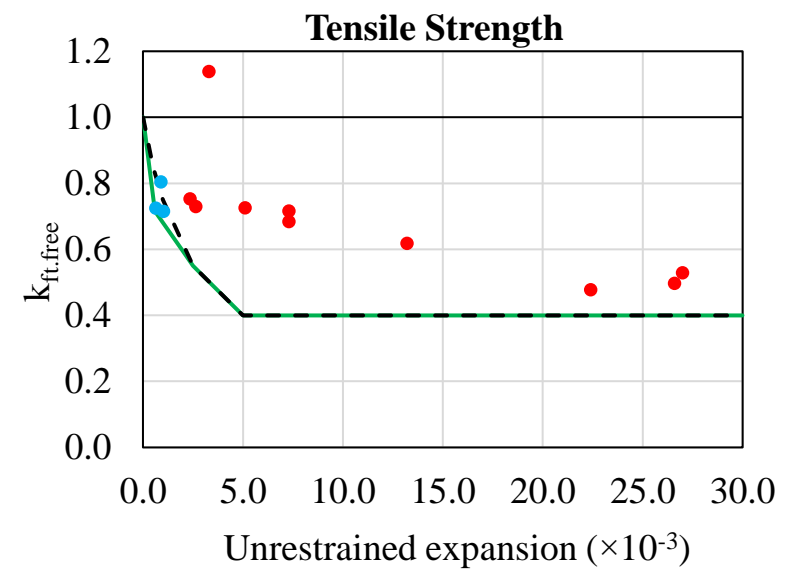
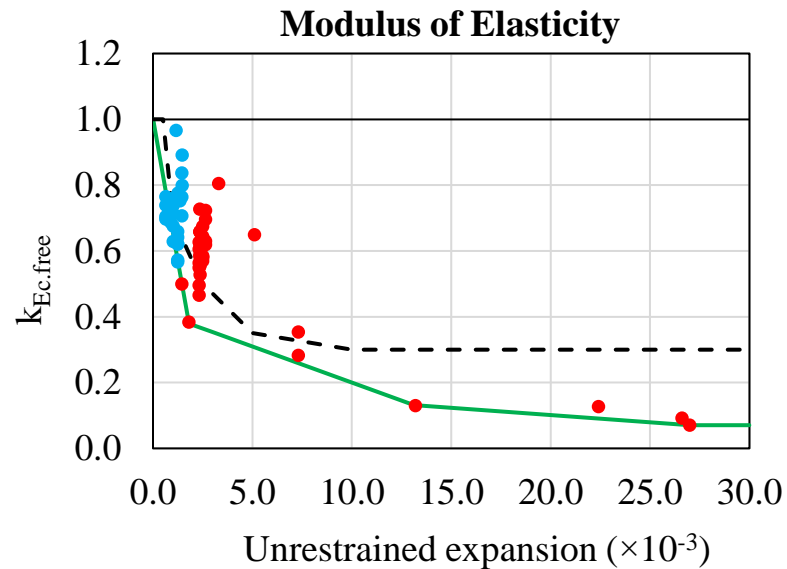
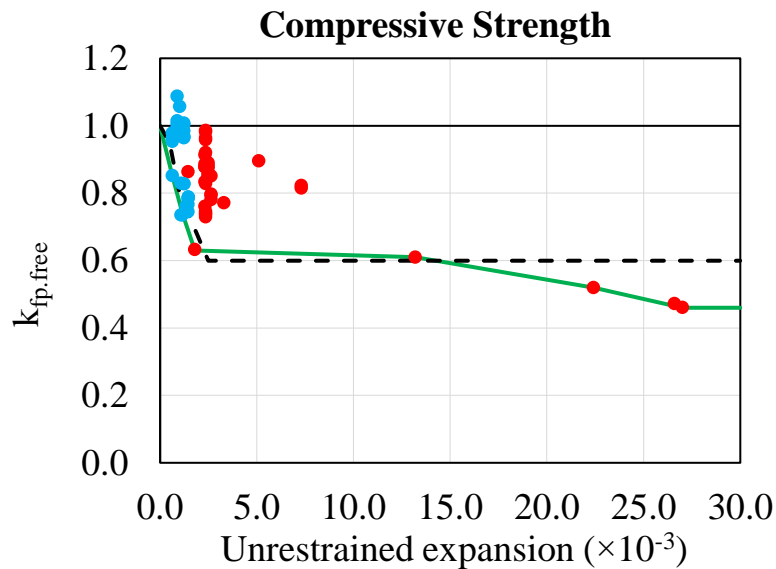
f_p : compressive strength
 ϵ_p : strain at peak stress
 E_c : modulus of elasticity
 f_{sp} : splitting tensile strength
 μ : Poisson's ratio

2. MECHANICAL PROPERTIES OF ASR-AFFECTED CONCRETE

MODEL FOR THE MECHANICAL PROPERTIES OF ASR-AFFECTED CONCRETE



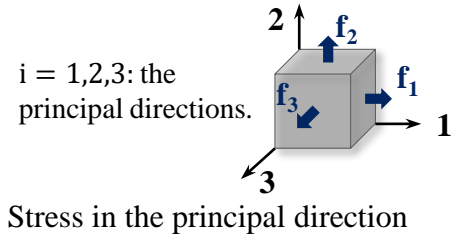
Modification factors for long-term stress-free condition



2. MECHANICAL PROPERTIES OF ASR-AFFECTED CONCRETE

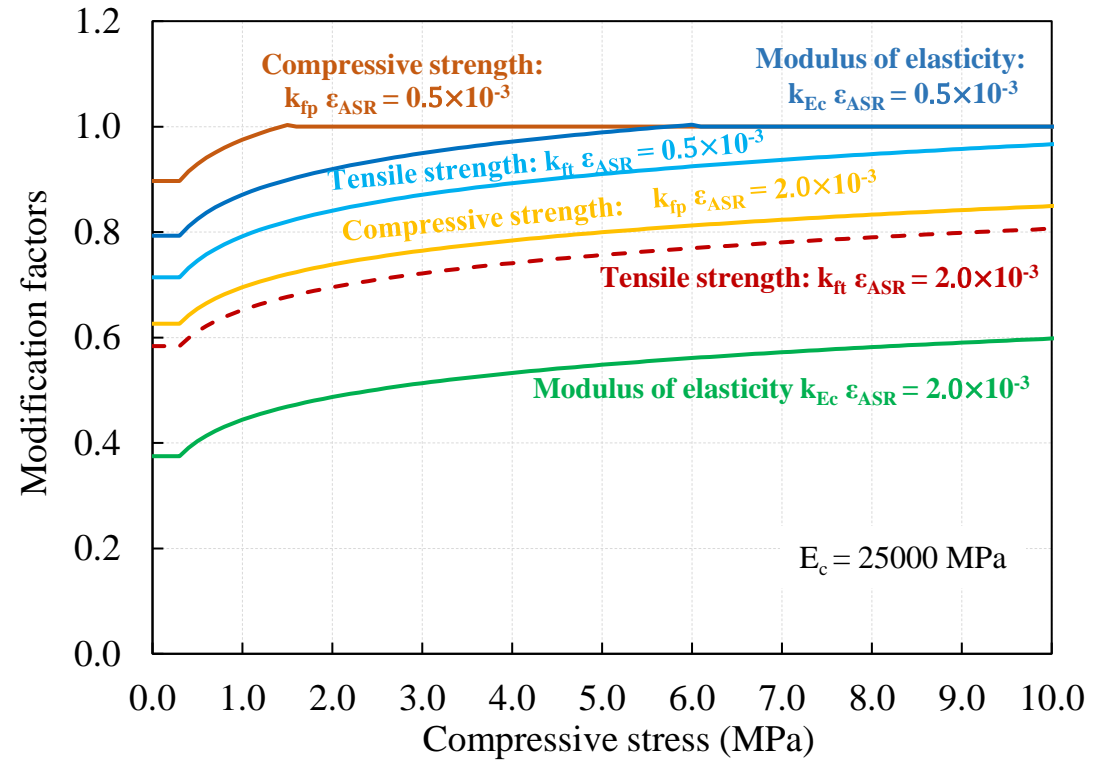
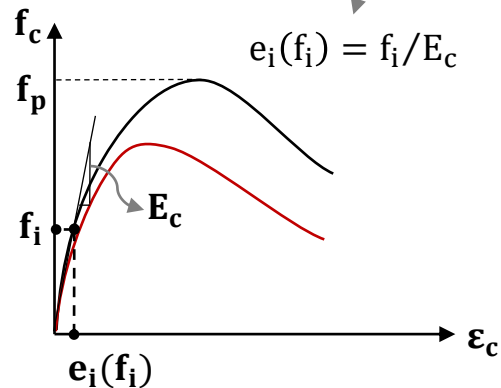
MODEL FOR THE MECHANICAL PROPERTIES OF ASR-AFFECTED CONCRETE

Modification factors for long-term restrained condition



$$k_{j,i}(f_i) = k_{j,i,free} + \frac{1}{1.05 \cdot \left(-\frac{\epsilon_{ASR}}{e_i(f_i)}\right)^{0.09}} - \frac{1}{1.05 \cdot \left(-\frac{\epsilon_{ASR}}{e_i(0)}\right)^{0.09}}$$

$j = f_p, E_c, f_t$



Isotropic Model

$$f_{p, isotropic} = \frac{(k_{fp,1} + k_{fp,2} + k_{fp,3})}{3} \cdot f_p$$

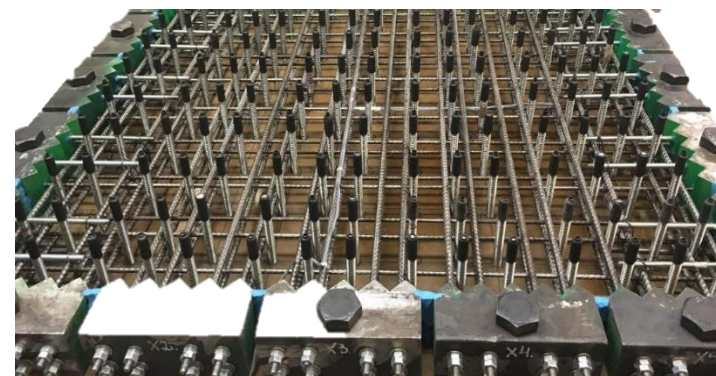
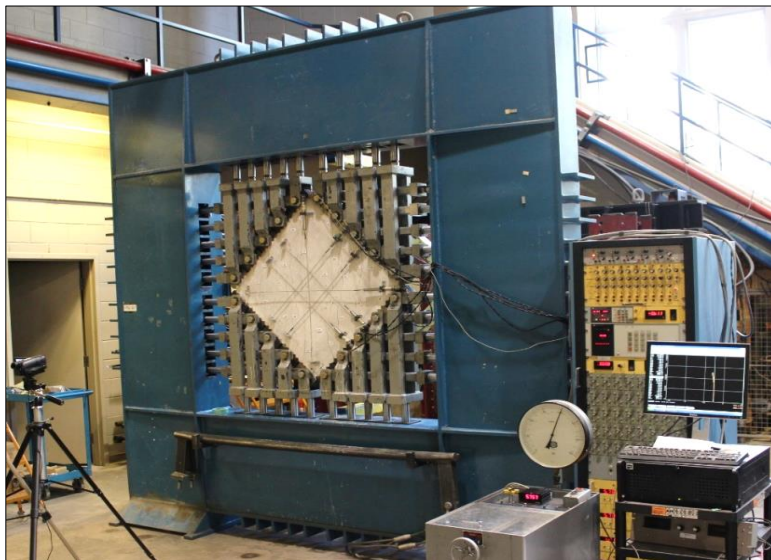
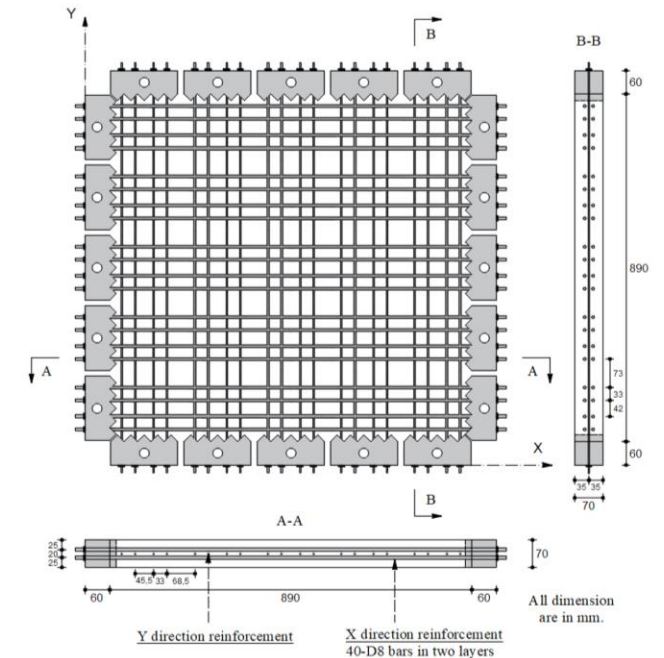
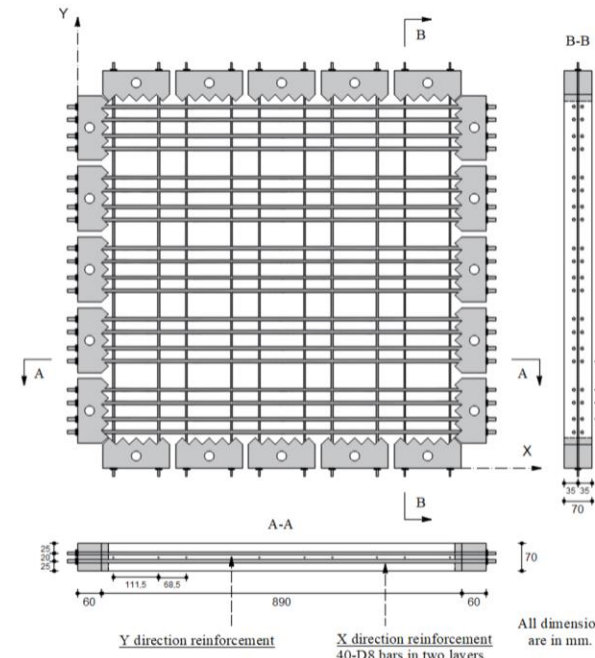
$$E_{c, isotropic} = \frac{(k_{Ec,1} + k_{Ec,2} + k_{Ec,3})}{3} \cdot E_c$$

$$f_{t, isotropic} = \frac{(k_{ft,1} + k_{ft,2} + k_{ft,3})}{3} \cdot f_t$$

3. VALIDATION STUDIES

ASR-AFFECTED SHEAR-CRITICAL ELEMENTS

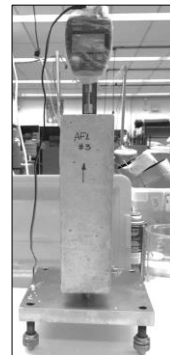
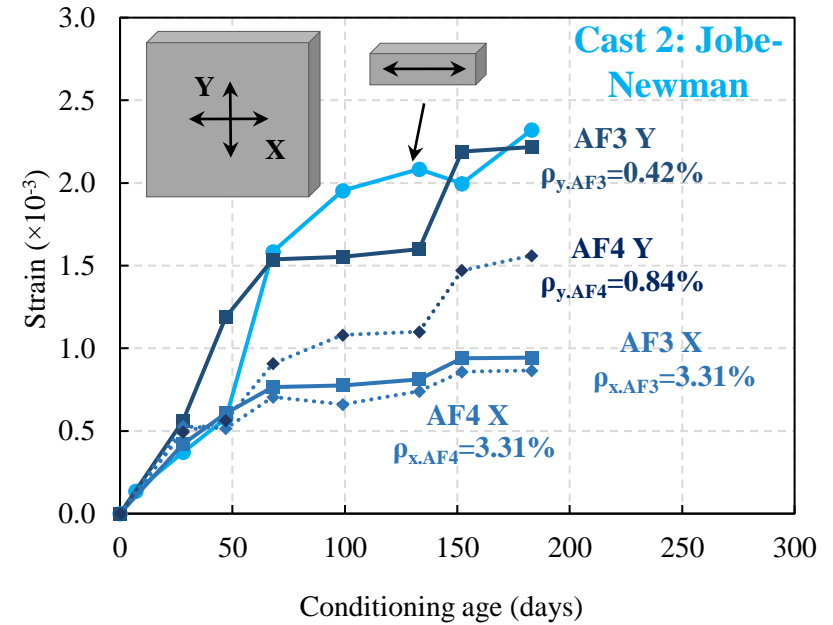
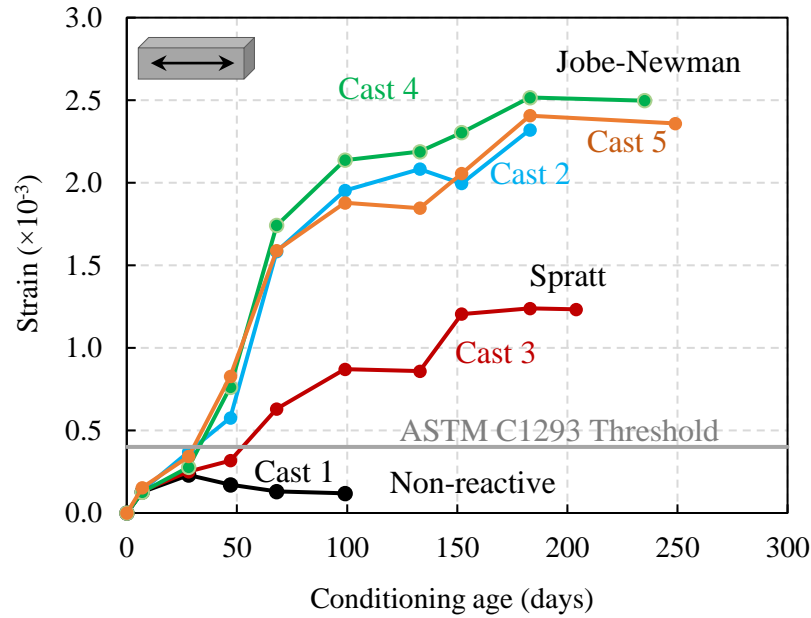
Cast no.	Specimen	ρ_x (%)	ρ_y (%)	ρ_z (%)	Reactive agg.	Loading
1	AF1	3.31	0.42	-	None	Monotonic
	AF2	3.31	0.84	-		
2	AF3	3.31	0.42	-	Jobe-Newman	Monotonic
	AF4	3.31	0.84	-		
3	AF5	3.31	0.42	-	Spratt	Monotonic
	AF6	3.31	0.84	-		
4	AF7	3.31	0.42	1.69	Jobe-Newman	Monotonic
	AF8	3.31	0.84	1.69		
5	AF9	3.31	0.20	-	Jobe-Newman	Monotonic
	AF10	3.31	1.66	-		



3. VALIDATION STUDIES

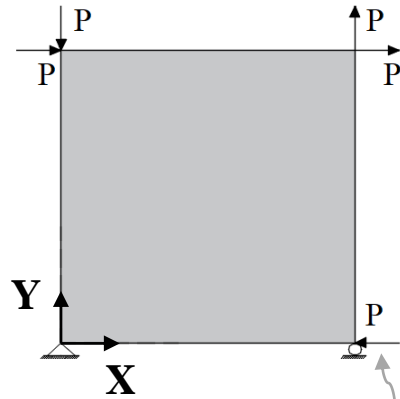
ASR-AFFECTED SHEAR-CRITICAL ELEMENTS

Expansion Monitoring



3. VALIDATION STUDIES

ASR-AFFECTED SHEAR-CRITICAL ELEMENTS



Force-controlled nodal load

FEA Concrete Properties Inputs			
$\epsilon_{ASR} (\times 10^{-3})$	required input	$C_c (^\circ C)$	$10 \times 10^{-6}^\dagger$
f_p (MPa)	required input	Max. agg. size (mm)	10
f'_t (MPa)	$0.33\sqrt{f'_c}^\dagger$	Density (kg/m ³)	2400 [†]
E_c (MPa)	$3320\sqrt{f'_c} + 6900^\dagger$	K_c (mm ² /s)	1.2 [†]
$\epsilon_o (\times 10^{-3})$	$1.8 + 0.0075 \times f'_c^\dagger$	S_x (mm)	1000 [†]
μ	0.15 [†]	S_y (mm)	1000 [†]

[†] Default properties assumed by VecTor2.

ASR Analyses

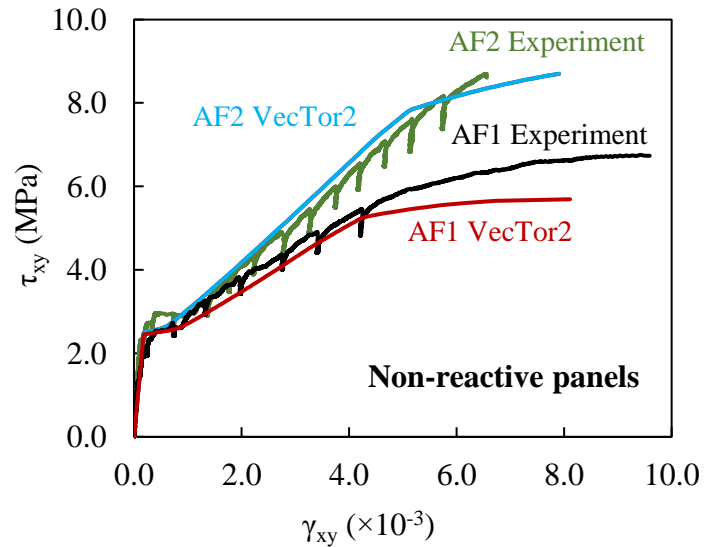


Concrete mechanical properties:

1. f_p at test day from reactive cylinders → **Cylinder at test day**
2. f_p at test day from non-reactive cylinders + anisotropic model → **Anisotropic**
3. f_p at test day from non-reactive cylinders + isotropic model → **Isotropic**



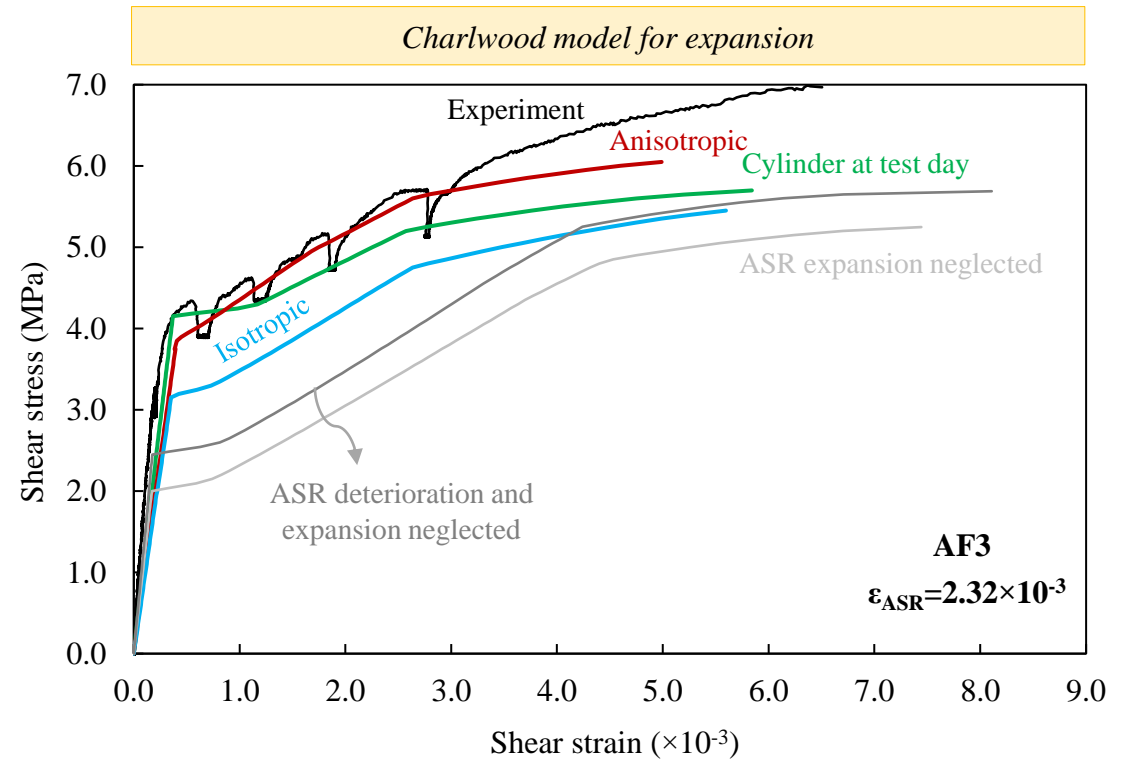
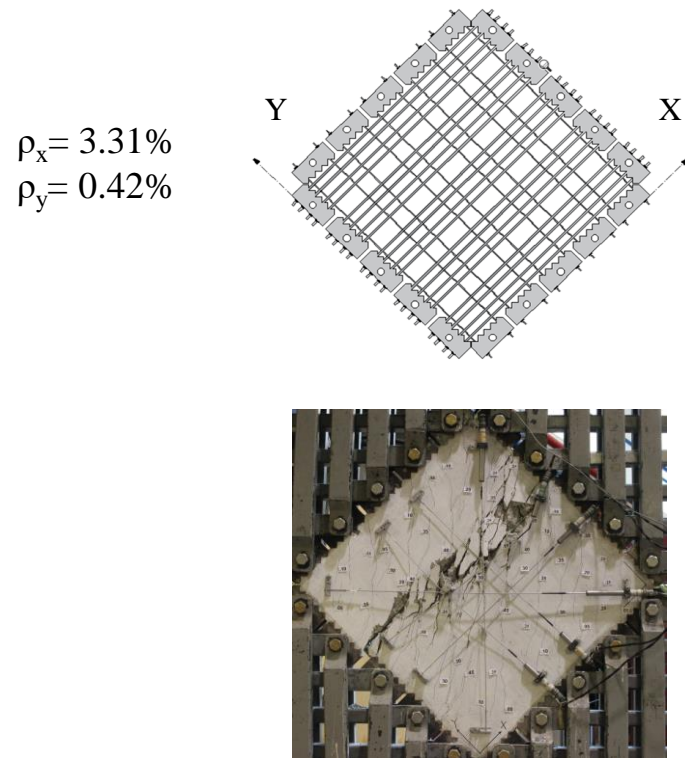
Charlwood model for expansion



3. VALIDATION STUDIES

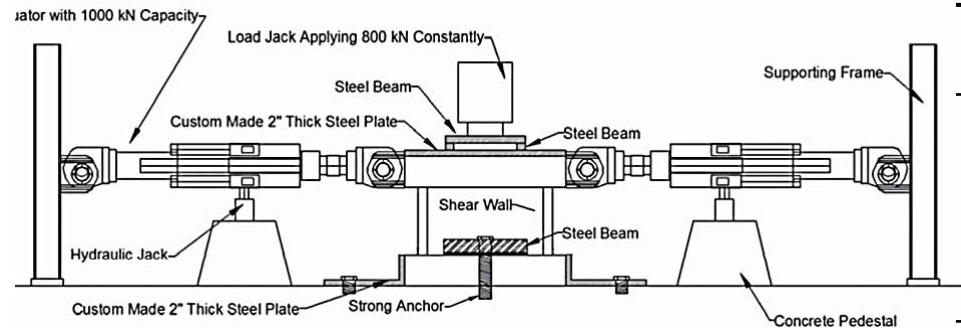
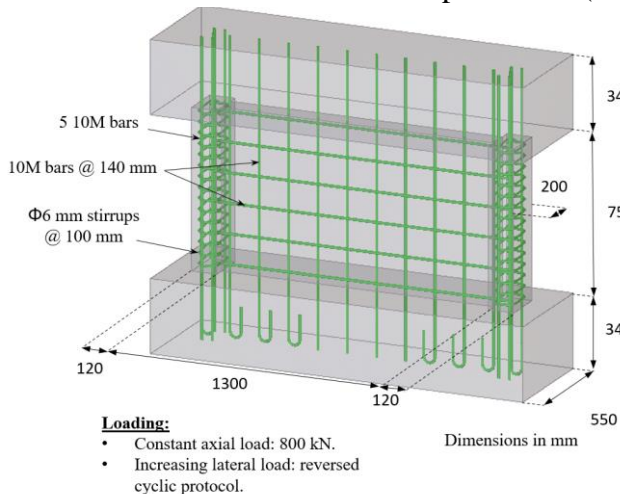
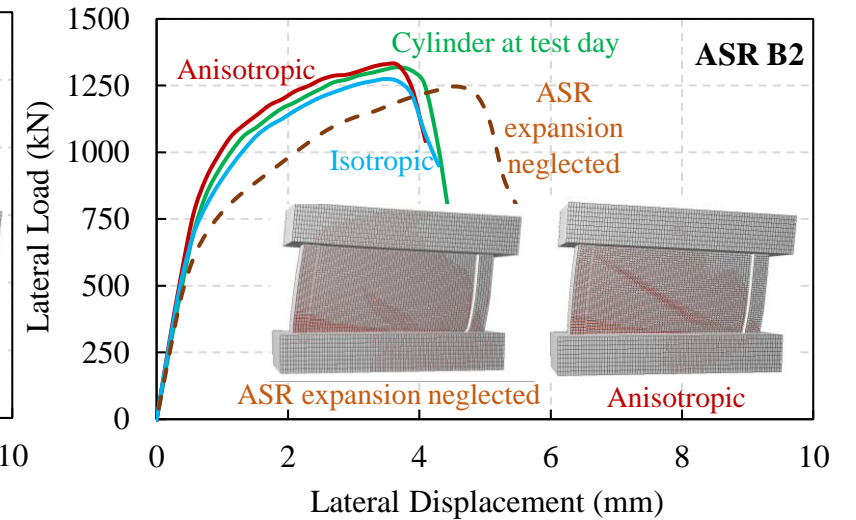
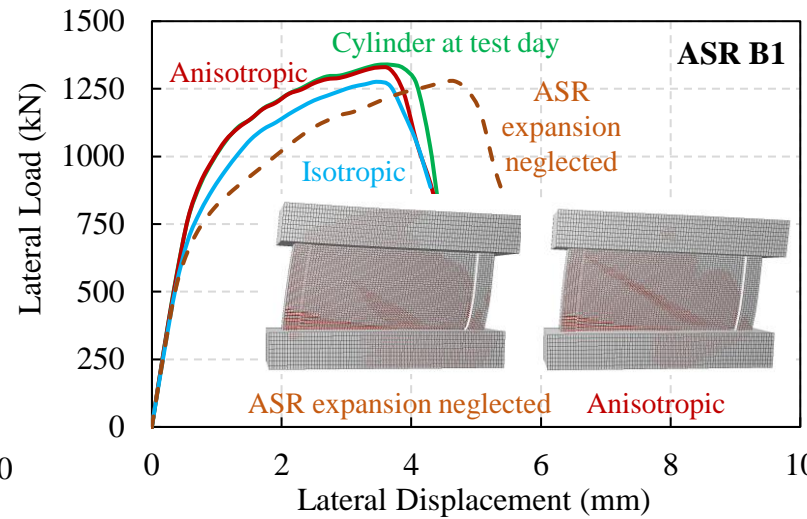
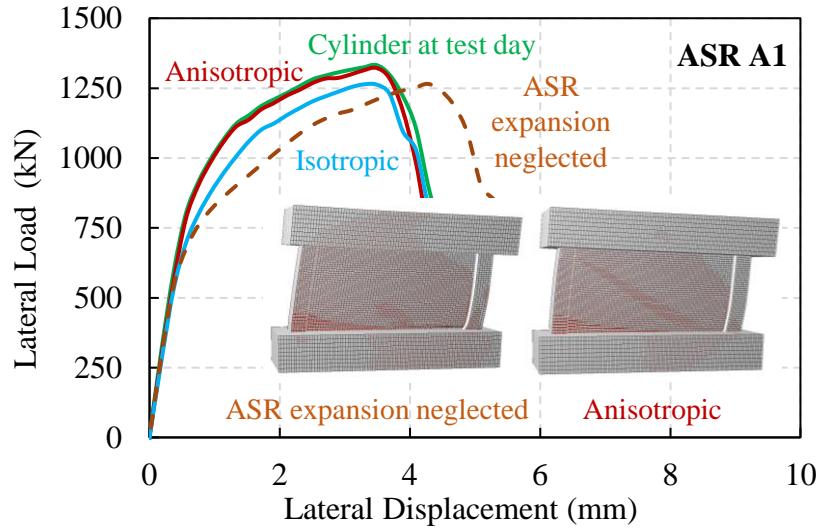
ASR-AFFECTED SHEAR-CRITICAL ELEMENTS

Panel Specimen AF3



3. VALIDATION STUDIES

ASR-AFFECTED SHEAR WALLS

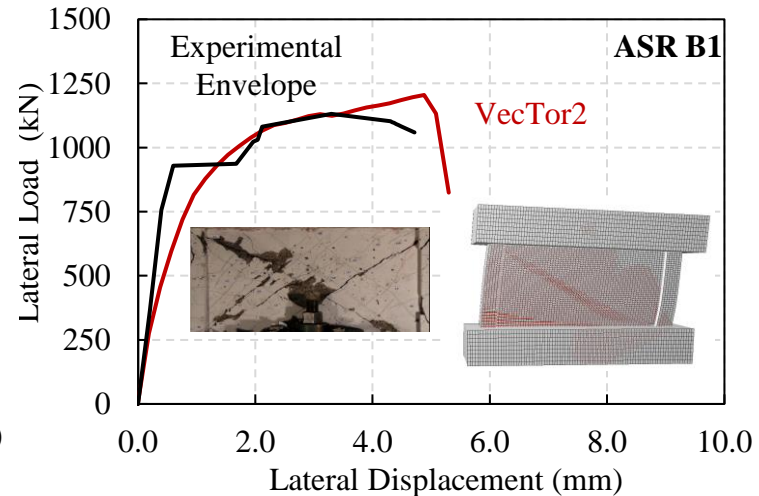
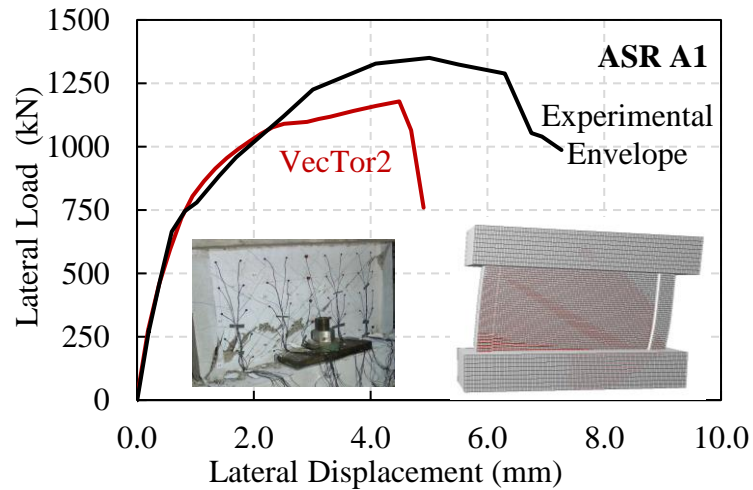
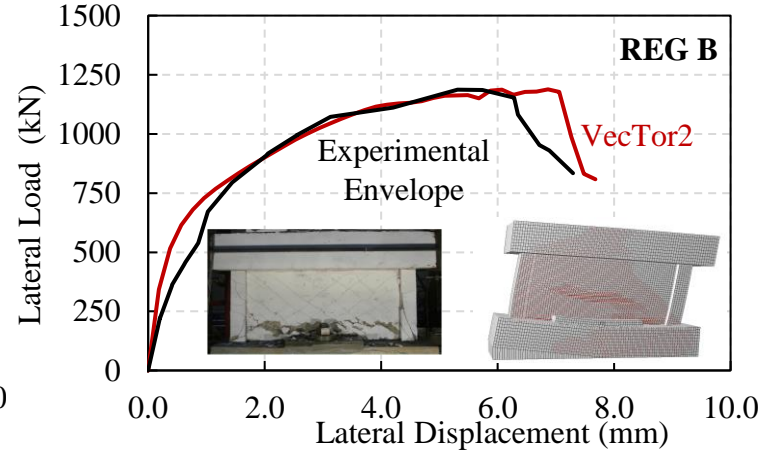
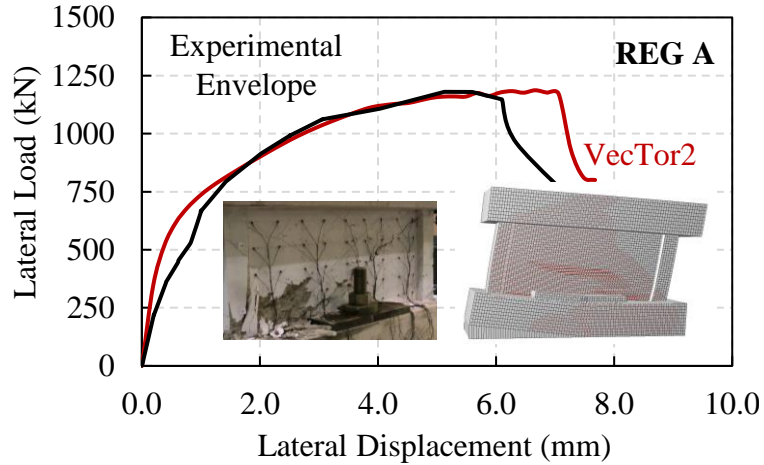


Specimen	f'_c (MPa)	E_c (MPa)	$\epsilon_{ASR} (\times 10^{-3})$	Age (days)
REG A	79.0	47150	---	240
ASR A1	63.7	35750	1.90	260
ASR B1	67.1	32600	2.15	610
ASR B2	63.0	28100	2.23	995
REG B	80.1	46652	---	975

†Tested by Habibi, F., Sheikh, S. A., Vecchio F. J., and Panesar, D. “Effects of Alkali-Silica Reaction on Concrete Squat Shear Walls,” *ACI Structural Journal*, V. 115, No. 5, 2018, pp. 1329-1339.

3. VALIDATION STUDIES

ASR-AFFECTED SHEAR WALLS

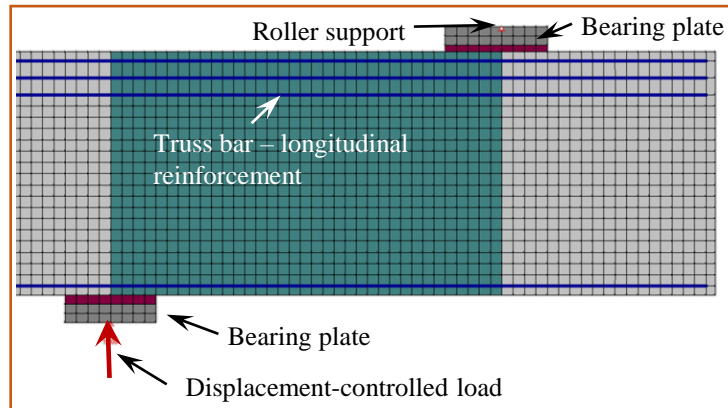
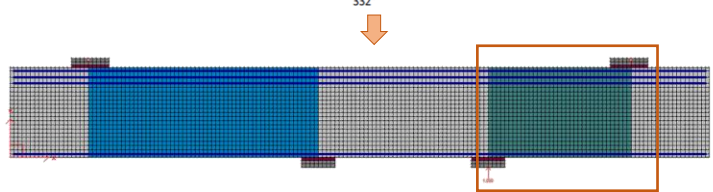
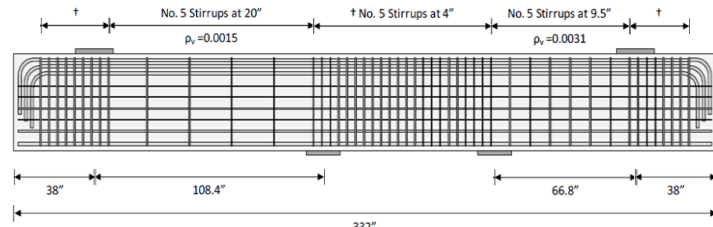


Specimen	$P_{u.Calc}$ (kN)	$P_{u.Exp}$ (kN)	$\delta_{u.Calc}$ (mm)	$\delta_{u.Exp}$ (mm)	$P_{u.Calc} / P_{u.Exp}$	$\delta_{u.Calc} / \delta_{u.Exp}$
REG A	1172	1180	7.00	6.10	0.99	1.15
REG B	1178	1187	7.06	6.30	0.99	1.12
ASR A1	1180	1355	4.50	6.20	0.87	0.73
ASR B1	1205	1240	4.88	4.90	0.97	1.00
ASR B2	1187	1243	4.60	2.60	0.95	1.77
Mean					0.96	1.15
COV (%)					4.72	29.8

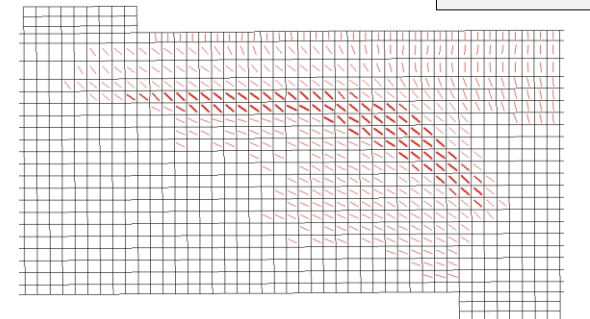
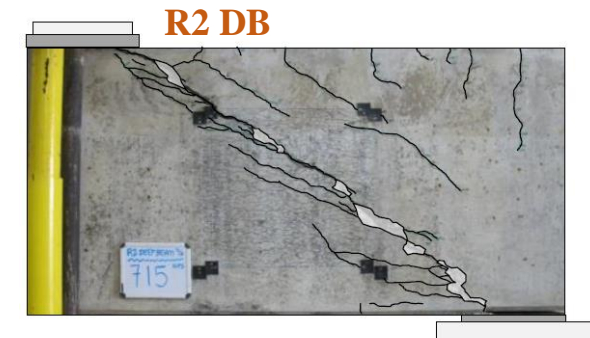
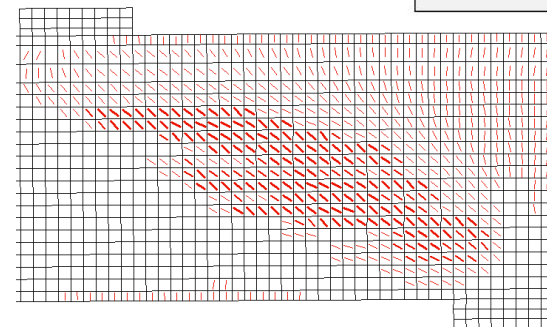
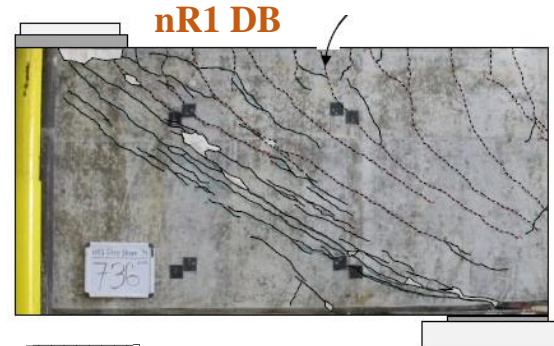
†Tested by Habibi, F., Sheikh, S. A., Vecchio F. J., and Panesar, D. “Effects of Alkali-Silica Reaction on Concrete Squat Shear Walls,” *ACI Structural Journal*, V. 115, No. 5, 2018, pp. 1329-1339.

3. VALIDATION STUDIES

SHEAR-CRITICAL BEAM SPECIMENS



Specimen	f'_c (MPa)	ϵ_{ASR} ($\times 10^{-3}$)	$V_{u.test}$ (kN)	$V_{u.calc}$ (kN)		$V_{u.calc} / V_{u.test}$	
				Cylinder	Anisotropic	Cylinder	Anisotropic
nR1 DB	50.3	---	2500	2105		0.84	
R1 DB	31.7	0.90	2309	2202	2155	0.95	0.93
R2 DB	27.0	4.40	2440	2692	2590	1.10	1.06
nR1 SS	49.6	---	1230	1440		1.17	
R1 SS	31.0	1.70	1496	1627	1530	1.09	1.02
R2 SS	29.0	6.30	1570	1409	1644	0.90	1.05

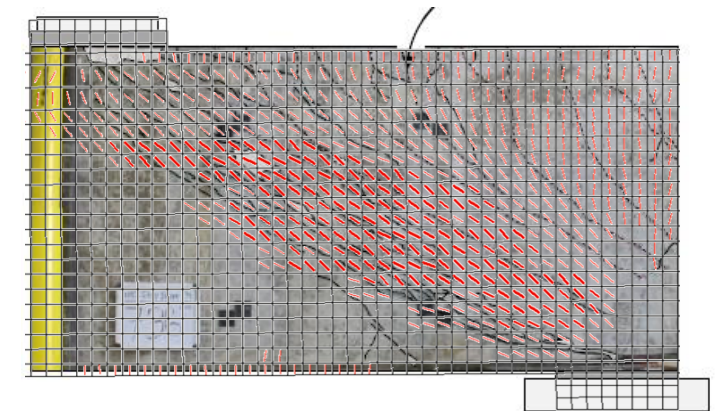
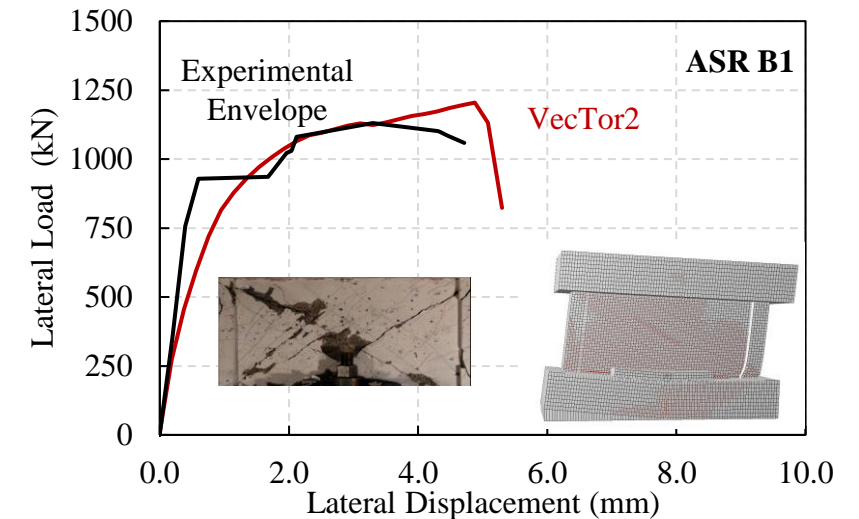


†Tested by Deschenes, D. J., Bayrak O., and Folliard, K.J. “ASR/DEF – Damaged bent caps: shear tests and field implications,” Technical Report for the Texas Department of Transportation, 2009, 271 pp.

4. CONCLUSIONS

The proposed anisotropic model for the mechanical properties of concrete results in the most accurate predictions of the overall response of the panels.

The similarity of the analytical responses obtained using either concrete properties determined from reactive cylinders or the anisotropic model for concrete properties indicates that, for an ASR-affected structure in the field, material information from either damaged or undamaged concrete can be used as valuable information for numerical analysis.



Ferche, A. C. and Vecchio, F. J. (2022) "Modeling of ASR-Affected Shear-Critical Reinforced Concrete Structures." *ACI Structural Journal* 119 (2), 75-88.

Ferche, A. C. and Vecchio, F. J. (2022) "Mechanical Properties of ASR-Affected Concrete." *ACI Materials Journal* 119 (1), 251-262.

Ferche, A. C. and Vecchio, F. J. (2021) "Behavior of ASR-Affected Reinforced Concrete Elements Subjected to Shear," *ACI Structural Journal*, No. 118, No. 4, pp. 163-174.

Ferche, A. C., Panesar, D. K., Sheikh, S. A., and Vecchio, F. J. (2017) "Toward Macro-Modeling of Alkali-Silica Reaction-Affected Structures," *ACI Structural Journal*, V. 114, No. 5, pp. 1121-1129

THANK YOU

